CYGNSS Storm-Centric Tropical Cyclone Gridded Wind Speed Product

DAVID R. MAYERS,[a] CHRISTOPHER S. RUF,[b] AND APRIL M. WARNOCK[a]

[a] *SRI International, Ann Arbor, Michigan*
[b] *University of Michigan, Ann Arbor, Michigan*

(Manuscript received 7 April 2022, in final form 12 December 2022)

ABSTRACT: The Cyclone Global Navigation Satellite System (CYGNSS) mission has generated several new ocean surface data products. Because of its high overpass rate and ability to measure surface wind speeds through weather, these data products are typically higher temporal resolution than traditional satellite tropical cyclone (TC) data products. However, the nature of the Global Navigation Satellite Systems reflectometry (GNSS-R) signal, which is essentially a single pixelwide measurement along the CYGNSS specular point (SP) track on the ground, necessitates aggregating the wind speed data over a period of time to accurately characterize TCs in terms of intensity and structure. The standard CYGNSS level 3 (L3) wind products are averaged over 1 h, which typically is not sufficient to produce an accurate characterization. A new L3 storm-centric gridded (SCG) wind speed product is presented here. It has been developed to improve upon the standard L3 algorithm for the purpose of providing better characterization of TC wind fields over their storm life cycle. This paper describes the L3 SCG algorithm, provides examples of L3 SCG wind fields, and discusses the potential uses and limitations of the new data product.

KEYWORDS: Hurricanes/typhoons; Radars/radar observations; Remote sensing; Satellite observations

1. Introduction

Accurate characterization of tropical cyclone (TC) winds, with regard to both intensity and structure, is necessary to improve storm forecasting. The Cyclone Global Navigation Satellite System (CYGNSS) mission was launched in late 2016 with the goal of improving TC wind characterization via two primary strategies: deployment of a constellation of minisatellites allowing for more frequent sampling than traditional satellite systems, and the use of Global Navigation Satellite Systems reflectometry (GNSS-R), which relies on signals of opportunity. GNSS-R measures surface properties via the L band, which enables the signal to penetrate intense rainbands in a TC inner core and measure the most intense wind speeds near the surface, while the use of signals of opportunity requires only a relatively lightweight and low-cost receiver for each satellite. The benefits of the CYGNSS mission's data have been investigated and demonstrated (Al-Khaldi et al. 2020; Cui et al. 2019; Ruf et al. 2019; Li et al. 2020; Mueller et al. 2021). However, one challenge to utilizing CYGNSS data for TC applications has been determining optimal methods for exploiting the mission's unique and irregular sampling pattern. The native (level 1) along-track data products are composed of pixelwide CYGNSS specular point (SP) tracks that vary in spatial resolution and overpass return rate depending on the latitude and inclination angle between the CYGNSS receiver and GNSS signal (Ruf et al. 2018). Figure 1 demonstrates typical overpass coverage of the eight CYGNSS satellites, each measuring four SP tracks, over 1 h (Fig. 1a), 12 h (Fig. 1b), and a full day (Fig. 1c). Wind speed is derived from CYGNSS using its level 1 Normalized Bistatic Radar Cross Section (NBRCS) measurements, which are mapped to ocean surface wind speeds using an empirical geophysical model function (GMF), resulting in the level 2 (L2) ocean surface wind speed products (Ruf and Balasubramaniam 2019). The standard level 3 (L3) gridded wind speed products are created from the CYGNSS SP along-track L2 wind speeds by aggregating the L2 winds for each of the four CYGNSS SP tracks, measured by each of the eight satellites in the constellation (32 total measurements each second), over an hourly window. Averaging and quality control (QC) are applied to the binned wind speeds, and the resulting wind speeds are gridded to a uniform 0.2° × 0.2° longitude–latitude grid. However, this standard product does not fully exploit the mission's advantageous data collection characteristics for representing TC winds for a given storm. One reason for this is that the 1-h averaging does not typically include enough CYGNSS SP tracks to adequately resolve the storms' intensity and structure. Second, this 1-h averaging results in few samples for determining CYGNSS SP track outliers, in both the cross- and along-track directions, making QC more difficult to perform. An additional complication is that when temporally averaging a TC wind field, the motion of the storm leads to "smearing" of the wind field. To circumvent this problem, wind speeds for TCs should be temporally averaged in a coordinate system that follows the motion of the storm (i.e., a storm-centric coordinate system). To illustrate this smearing effect, Fig. 2 shows a CYGNSS overpass of a TC over a 24-h duration. Many distinct CYGNSS SP tracks pass through the storm, and in this case, they are distributed well enough that some wind field structure can be seen. The left panel of Fig. 2, which has a concentrated region of high wind speeds near the center of the storm, is plotted in storm-centric coordinates; that is, the location of each wind speed sample is

Denotes content that is immediately available upon publication as open access.

Corresponding author: April Warnock, april.warnock@sri.com

DOI: 10.1175/JAMC-D-22-0054.1

© 2023 American Meteorological Society. For information regarding reuse of this content and general copyright information, consult the AMS Copyright Policy (www.ametsoc.org/PUBSReuseLicenses).

Brought to you by UNIVERSITY OF MICHIGAN | Unauthenticated | Downloaded 03/06/23 02:27 PM UTC

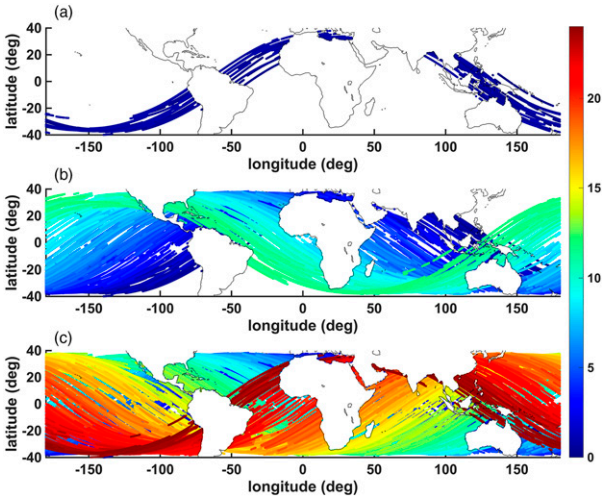


FIG. 1. Example of CYGNSS L2 sampling over (a) 1, (b) 12, and (c) 24 h. Data shown are from 27 Nov 2021 v3.1 SDR. Samples are colored by collection time, in hours from 0000 UTC.

adjusted to account for the movement of the storm. By contrast, the right panel of Fig. 2 contains aggregated CYGNSS SP tracks that have been plotted in the native geophysical coordinate system, not accounting for the storm's motion, leading to the wind field appearing smeared as the storm moves over the time window.

To address the shortcomings of the standard CYGNSS L3 gridded wind product for characterizing individual TC wind fields, we have developed an alternative gridded wind speed product that employs a longer averaging period in a storm-centric coordinate system, implements additional CYGNSS SP cross-track averaging and QC algorithms, and outputs the winds for a standard 7.2° × 7.2° region surrounding a storm's center location. The overarching goal of this algorithm is to provide storm-specific, user-friendly wind fields that better characterize storm structure and intensity and filter out less reliable data points. This version of the L3 wind speeds is referred to the L3 Storm-Centric Gridded (SCG) wind speed product. This paper details the algorithm development of the L3 SCG product in section 2, presents examples of the L3 SCG wind speeds in section 3, and closes the article with a discussion and summary of the L3 SCG product in section 4.

2. L3 storm-centric gridded algorithm

A high-level overview of the L3 SCG algorithm is shown in the flowchart in Fig. 3. The first step of the algorithm combines CYGNSS SP track-based wind speeds as reported in the CYGNSS L2 files, aggregated over a standard 7.2° × 7.2° spatial grid and ±6-h temporal averaging window centered on the storm's location, which is estimated from TC best-track data interpolated to the center of the L3 SCG time window. This results in an intermediate wind field with collocated wind speeds on a storm-centric grid coordinate system. A schematic of the storm-centric grid coordinate system is shown in Fig. 4, where the origin of the coordinate system is defined by the storm center location, r is the radius from the storm's center, and θ is the polar angle, defined as positive counterclockwise from east. Next, several QC processes are implemented to remove questionable values. The QC processes are described in detail below. The wind speeds remaining after the QC process are then averaged for each cell using an inverse variance weighting scheme (Ruf 2018). Repeating this process every 6 h throughout the storm's life cycle creates a time series of gridded wind speeds centered on the storm's path. The wind speeds are then reprojected back to geographic coordinates and output on a storm-by-storm basis that roughly covers the life cycle of the storm (depending on the time frame spanned by the resulting QCed wind fields). The files also include the

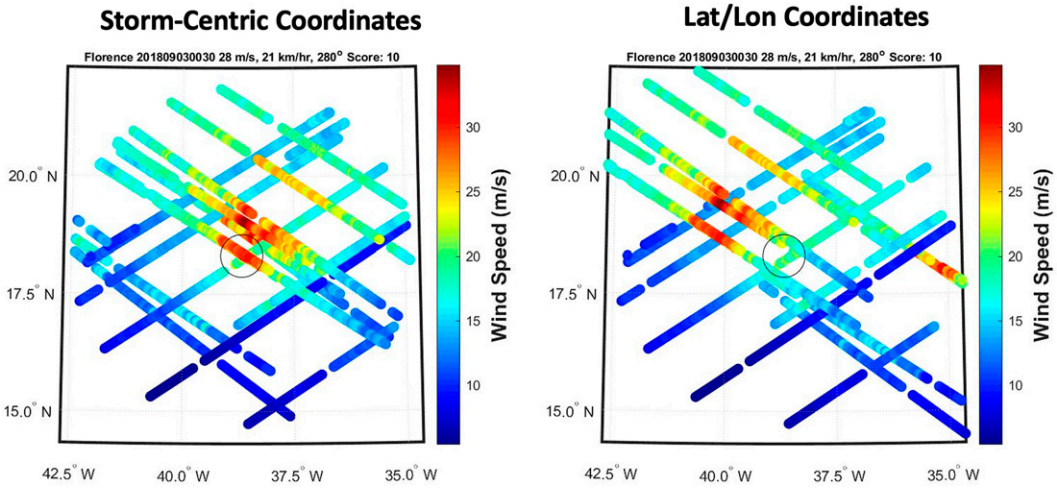


FIG. 2. CYGNSS wind speeds in Hurricane Florence from a 24-h duration starting at 0030 UTC 3 Sep 2018, (left) plotted in storm-centric coordinates and (right) plotted with the regular latitude–longitude of each wind speed. Wind speeds shown are from the v3.0 SDR L2 dataset. The black open circle represents the reported TC center location at the center of the 24-h period.

Brought to you by UNIVERSITY OF MICHIGAN | Unauthenticated | Downloaded 03/06/23 02:27 PM UTC

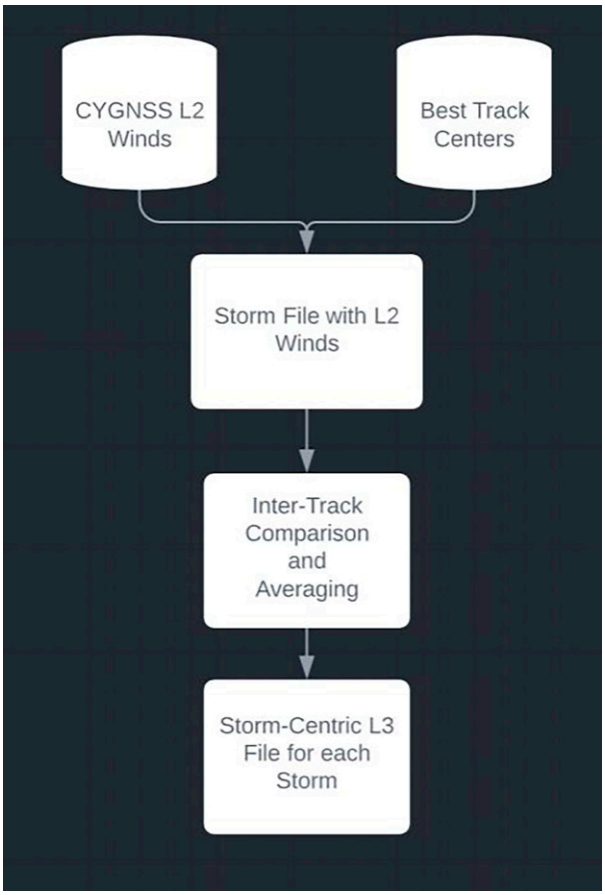


FIG. 3. Flowchart of the basic L3 SCG algorithm. The storm file with L2 winds contains the L2 winds in a polar coordinate system. The winds are converted to storm-centric coordinates for the QC and averaging and are reprojected to a lat–lon grid for the final product. The files also include the final wind fields on a polar coordinate grid.

wind fields on a polar coordinate grid, as may be required by some end users.

a. Inputs

Both the standard L3 gridded wind speed product and the L3 SCG wind speed products derive their gridded winds from the most recent release (V3.1) of the L2 Science Data Record (SDR) products (Pascual et al. 2021). For the standard product, all wind speeds generated in a single L2 file (covering a 24-h period) are inputs to the L3 gridding algorithm. The standard L3 product reports two wind speed products: a fully developed seas (FDS) wind speed product, and a young seas/limited fetch (YSLF) wind speed product. These two wind fields address the need for differing wind speed derivation algorithms based on low-to-moderate and high winds, respectively. For the L3 SCG, the focus on TCs specifically necessitates the use of the YSLF wind speeds to the algorithm.

In addition to the L2 YSLF wind speeds, a time-continuous storm center location is required to compute relative latitude and longitude coordinates for each sample. To approximate

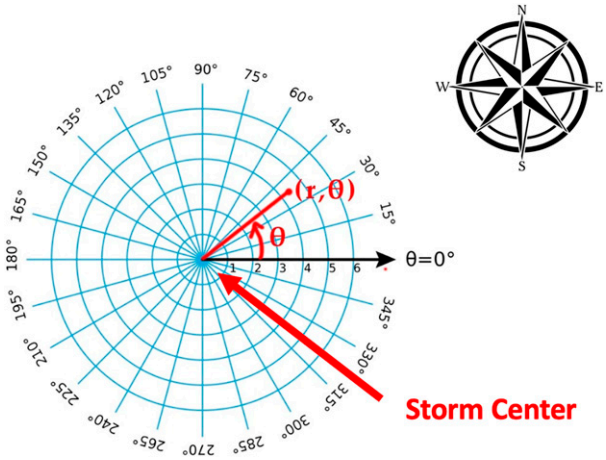


FIG. 4. Storm-centric coordinate system; the origin is defined by the storm's center location at the reporting time, r is the radius from the storm's center (km), and θ is the polar angle, which is positive counterclockwise from east.

this, best-track TC storm centers (available at primary synoptic hours) are linearly interpolated. These data are not known a priori and must be supplied by an ancillary data source. In the current version of the algorithm TC best-track data reported in the National Hurricane Center (NHC) best-track dataset (Landsea and Franklin 2013) is used for TCs in the Northern Atlantic and east Pacific basins, and the Joint Typhoon Warning Center (JTWC) database is used for storms occurring in the western Pacific, Southern Hemisphere, and north Indian Ocean. Alternatively, preliminary TC track data with a lower latency period such as from the Automated Tropical Cyclone Forecast (ATCF) b-decks provided by the NHC or the International Best Track Archive for Climate Stewardship database (IBTrACS; Knapp et al. 2010, 2018) can be used to create L3 SCG files in near–real time. The dataset discussed herein, however, uses the official best-track locations to optimize the accuracy of the L3 SCG products.

b. Averaging windows

Well-chosen bounds need to be placed on the spatial and temporal sampling windows to balance the trade-off between a greater number of samples per grid cell (obtained with longer/larger temporal/spatial windows) that enable CYGNSS SP intertrack comparison and quality control, and data processing errors that dominate larger averaging periods/windows. If the spatial bounds are too wide (the gridcell size is large relative to the features of the TC wind field), wind speed measurements from very different parts of the storm are compared and potentially averaged together. This scenario will result in too much data being thrown out as a result of poor CYGNSS SP intertrack comparisons, and the storm structure will be washed out by a coarse spatial resolution of the wind speed product. A spatial averaging window of 0.8° has been found to provide a good balance between the number of wind speeds in each L3 SCG grid cell and preventing loss of information in the wind field. Figure 5 shows a schematic of the reporting

Brought to you by UNIVERSITY OF MICHIGAN | Unauthenticated | Downloaded 03/06/23 02:27 PM UTC

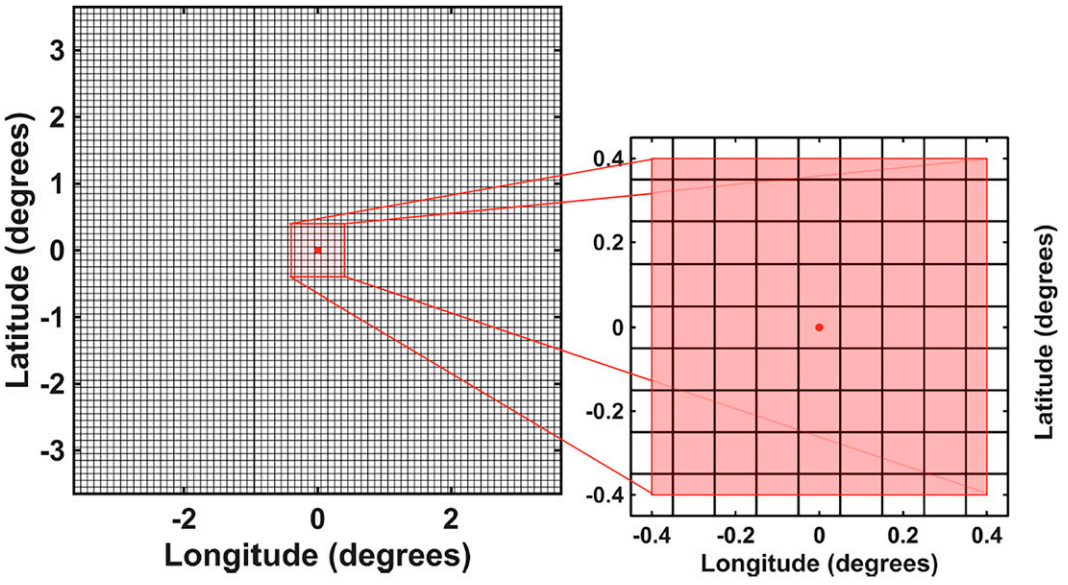


FIG. 5. (left) Schematic of the entire 7.2° × 7.2° grid for a given wind field, and (right) the spatial averaging implementation for a single grid point. The black grid denotes the 0.1° × 0.1° reporting grid. The red dot is the center of an arbitrary grid cell, and the red square represents the spatial averaging window, i.e., the 0.8° × 0.8° area from which this grid cell derives its CYGNSS samples for calculating the cell's averaged wind speed.

grid cells with 0.1° × 0.1° resolution (black grid), relative to an L3 SCG grid-cell center (red dot) and the spatial averaging window (red box). For each grid cell, samples are taken from the spatial averaging window, a ±0.4° latitude–longitude box centered on the grid cell, to populate the cell. This leads to some overlap between cells, that is, the same CYGNSS samples are used in multiple grid cells.

The temporal averaging window defines the duration over which samples are combined to provide a single wind speed estimate for each cell. The temporal averaging window should be large enough to obtain an adequate number and distribution of samples for CYGNSS SP intertrack comparisons, but not so large that the TC changes significantly within the averaging window. A 12-h temporal averaging window was chosen to best meet this objective. A wind speed grid is reported every 6 h, and each grid contains samples from ±6 h. This 12-h temporal averaging window maintains a Nyquist sampling rate (2 times rate of reporting vs resolution) and ensures that at least one overpass of the CYGNSS constellation will be included in the window (overpasses occur approximately 2 times per day). Some storms will have significant changes in their wind field over 12 h, especially storms that are rapidly intensifying; a caveat that users should keep in mind when using the data product for studies where short-term wind fields are necessary. Since many more storms do not change significantly over 12-h windows versus those that do, the longer averaging time frame was selected for the standard L3 SCG product algorithm.

In summary, each 6-hourly L3 SCG wind field grid is populated in storm-centric coordinates with a 12-h temporal averaging window, a 0.8° spatial averaging window, on a 0.1° grid. The combination of the larger spatial averaging window and the wider temporal window typically allows for multiple CYGNSS SP tracks to be present in each cell. Figure 6 shows a histogram of the number of samples used to calculate averages per grid cell for the L3 SCG products, using all data in year 2018. The histogram shows that the majority of the averaged wind values are calculated by averaging at least 20 data samples from 2 or more CYGNSS SP tracks. The standard L3 wind product, by contrast, typically averages 2–3 samples from a single CYGNSS SP track. The collocation of multiple CYGNSS SP tracks in the L3 SCG grids allows for intertrack comparisons and quality control that the standard L3 wind speed algorithm cannot apply due to lack of multiple CYGNSS SP tracks represented in an averaging cell.

c. *CYGNSS SP intertrack comparison and averaging*

The QC and averaging process for the L3 SCG algorithm consists of three steps: 1) An uncertainty upper bound cutoff, 2) CYGNSS SP intertrack consistency QC, and 3) inverse variance weighted averaging. The first process simply removes any data samples that are flagged in the input L2 data as having uncertainty values greater than 8 m s^{-1}. This is done as a first stage QC to remove questionable wind values from the final product. The choice of 8 m s^{-1} for the cutoff is based on trials varying the cutoff from 6 to 11 m s^{-1}, where 8 m s^{-1} was determined to be the threshold that retains the majority of the high storm wind samples while removing obviously noisy data values. The impact of this QC step is shown in Fig. 7, which demonstrates the typical relationship between the L2 wind speeds and their associated uncertainty values in the form of a scatterplot containing all L2 YSLF wind speeds over ~20 days of files. The plotted data include files with peak intensity winds from Hurricanes Dorian (2019), Michael

Brought to you by UNIVERSITY OF MICHIGAN | Unauthenticated | Downloaded 03/06/23 02:27 PM UTC

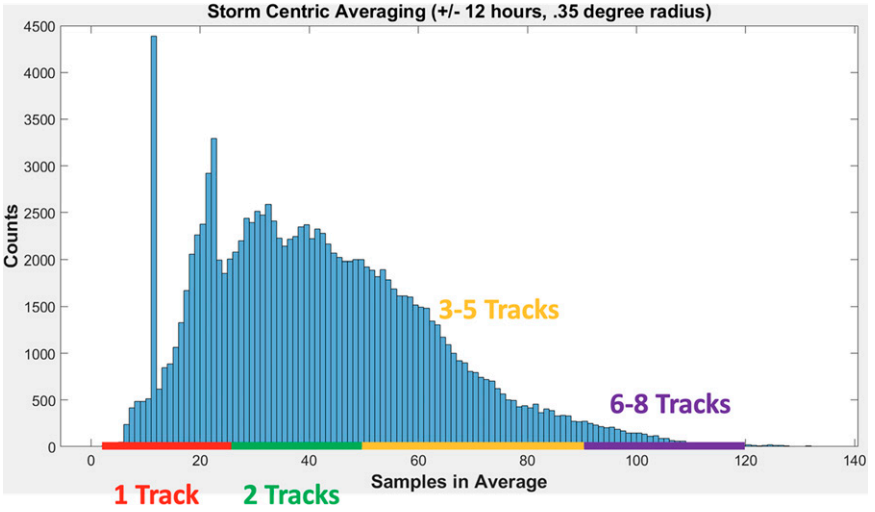


FIG. 6. Histogram of the number of samples per averaging cell for the L3 SCG algorithm. There are typically >20 samples per average, vs the 2–3 samples typically represented in the standard L3 algorithm. The spike at about 11 samples/track is likely due to this number being the average number of samples in a single track that fall within a 0.8° × 0.8° spatial window.

(2018), Laura (2020), and Sam (2021), to ensure that very high wind speeds are represented in the statistics. The >8 m s^{-1} uncertainty cutoff is highlighted as the dashed line. Wind speeds greater than tropical storm force (≥17.4 m s^{-1}) make up less than 3% of the wind speed samples. Of these, less than 4% of the samples have wind speed uncertainties of >8 m s^{-1}.

Next, CYGNSS SP intertrack comparisons are performed for each grid cell. This step is added to improve upon the standard L3 algorithm averaging process that primarily relies on CYGNSS SP along-track averaging due to the lack of numerous nearby CYGNSS SP tracks over the 1-hourly averaging period; CYGNSS SP along-track averaging reduces the effective spatial resolution of the reported wind speed while reducing noise in the measurement, but it does not control for bias in the CYGNSS SP track. Even when there are multiple CYGNSS SP tracks present in the standard L3 wind speed algorithm, there is no CYGNSS SP intertrack comparison to see if the CYGNSS SP tracks agree; the wind speeds from each CYGNSS SP track are simply averaged together using the inverse-variance weighted average. The CYGNSS SP intertrack QC for the L3 SCG products is conducted as a function of the number of CYGNSS SP tracks T represented in a cell. Each cell must contain wind speed samples from at least two CYGNSS SP tracks for a cell-averaged wind speed to be calculated. If there is only one CYGNSS SP track in a cell, then a consistency check is not possible as there is no way to verify that the wind speeds for that CYGNSS SP track are not problematic and hence the data point is thrown out. When there are two or more CYGNSS SP tracks in a grid cell, the

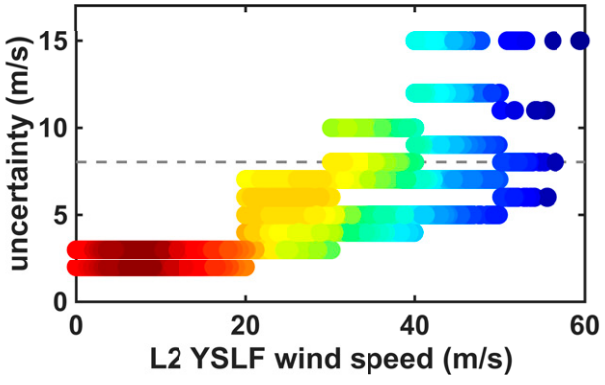


FIG. 7. Typical distribution of the L2 YSLF wind speeds and their associated uncertainties for ~20 days of L2 YSLF data. The gray dashed line highlights the maximum allowable uncertainty for the L3 SCG input winds. Wind speeds above this line would be thrown out during initial QC. The color scale represents the log relative density of points.

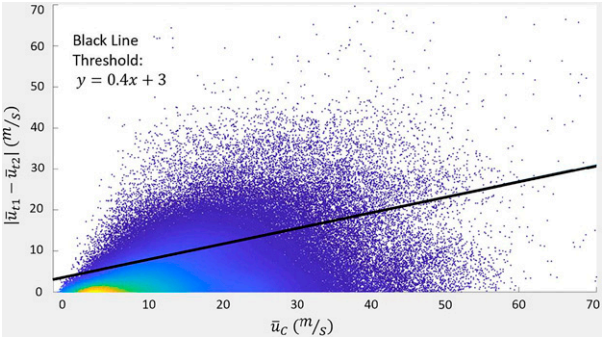


FIG. 8. Scatterplot of the difference between two mean CYGNSS SP track wind speeds vs the average wind speed of the cell for all storms in 2018. The black line is defined by Eq. (3) and indicates the threshold below which the two CYGNSS SP tracks are defined in agreement and used to calculate a wind speed for that cell. For these data, 80% of two-track cells are within the threshold.

Brought to you by UNIVERSITY OF MICHIGAN | Unauthenticated | Downloaded 03/06/23 02:27 PM UTC

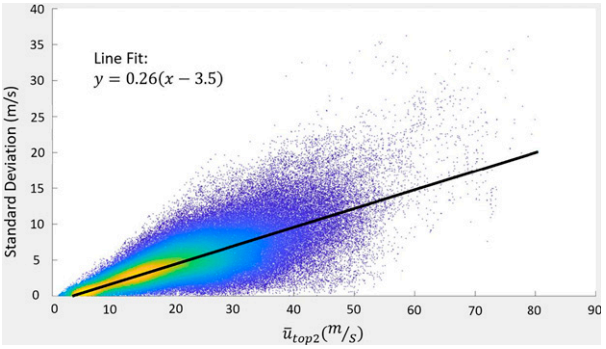


FIG. 9. The standard deviation of the mean CYGNSS SP track wind speeds ($\overline{u}_t$) plotted against the mean of the two highest mean CYGNSS SP track wind speeds for all 2018 storms. The line fit is used to estimate a typical standard deviation value given $\overline{u}_{\text{top2}}$. When there are three or more CYGNSS SP tracks in a cell, this relation is used to determine whether the CYGNSS SP tracks agree well enough to report an averaged wind speed for that cell.

mean CYGNSS SP track wind speed $\overline{u}_t$ is computed for each CYGNSS SP track. If there are N samples in the cell with N_t samples in the tth CYGNSS SP track, the mean CYGNSS SP track wind speed for the tth CYGNSS SP track is given by

$$\overline{u}_t = \frac{1}{N_t}\sum_{j=1}^{N_t} u_j, \tag{1}$$

where u_j is the wind speed of the jth sample in the tth CYGNSS SP track, and all wind speeds within a cell are averaged to give the mean cell wind speed $\overline{u}_C$:

$$\overline{u}_C = \frac{1}{N}\sum_{t=1}^{t=T} N_t \overline{u}_t. \tag{2}$$

For the case of $T = 2$, the mean CYGNSS SP track wind speeds $\overline{u}_t$ are compared to evaluate how well the CYGNSS SP tracks agree. It is expected that the difference between the two mean CYGNSS SP track wind speeds will be larger when higher wind speeds are present. To account for this and to establish a threshold over which the data point is discarded, the difference between the mean CYGNSS SP track wind speeds $|\overline{u}_{t1} - \overline{u}_{t2}|$ is compared with the mean cell wind speed $\overline{u}_C$. Figure 8 shows the relationship between the mean track wind speeds and mean cell wind speeds for all cells, over all storm files available in 2018. As expected, in Fig. 8 it is observed that the difference $|\overline{u}_{t1} - \overline{u}_{t2}|$ tends to increase with $\overline{u}_C$. As such, the threshold indicated on Fig. 8 (black line) was chosen to vary linearly with $\overline{u}_C$ to allow for a larger difference between CYGNSS SP tracks at high wind speeds. The threshold was defined to keep ~80% of the samples and discard the remaining 20%. These numbers are determined ad hoc in an attempt to retain the majority of samples while removing those with the most egregious disagreements between them. The threshold limit is given by

$$|\overline{u}_{t1} - \overline{u}_{t2}| < 0.4\overline{u}_C + 3. \tag{3}$$

All data points that meet the criteria in Eq. (3) are considered to be in sufficient agreement and the mean cell wind speed $\overline{u}_C$ is reported as Eq. (2). If there is a large difference between two CYGNSS SP tracks and the difference exceeds the threshold, no wind speed is reported for the cell.

When there are more than two CYGNSS SP tracks in a cell ($T > 2$), an outlier test is done to check if any mean CYGNSS SP track wind speeds $\overline{u}_t$ are anomalous. All samples are used when defining what is an outlier. The outlier definition is computed separately for each cell in the grid, and even if a sample is excluded from the average in one grid cell, it will still be considered for inclusion in other grid cells. The CYGNSS SP track x is not an outlier if its mean CYGNSS SP track wind speed is within $3x$ standard deviations of the mean cell wind speed computed without CYGNSS SP track x. This is represented by the condition

$$\overline{u}'_C - 3\sigma'_C < \overline{u}_x < \overline{u}'_C + 3\sigma'_C, \tag{4}$$

where the prime superscript indicates that CYGNSS SP track x is excluded when computing the term and where

$$\sigma'_C = \sqrt{\frac{1}{(T-1)-1}\sum_{t\neq x}|\overline{u}_t - \mu|^2} \quad \text{and} \tag{5}$$

$$\mu = \frac{1}{T-1}\sum_{t\neq x}\overline{u}_t. \tag{6}$$

Outlier CYGNSS SP tracks that are flagged by this method are removed from the averaging. The algorithm also checks to see if unique CYGNSS SP tracks of data are present in any particular 6-hourly increment of its implementation, to avoid an exact duplication of the SCG product from one 6-h increment to the next.

TABLE 1. Summary of differences between the standard CYGNSS L3 gridded wind speed product and the L3 SCG product.

	Std L3 wind speed product	L3 SCG wind speed product
Temporal averaging window	1 h (±0.5 h from reporting time)	12 h (±6 h from reporting time)
Spatial reporting interval	0.2° × 0.2°	0.1° × 0.1°
Inputs	L2 SDR V3.1 wind speeds from all 8 CYGNSS satellites; YSLF and FDS wind speeds	L2 SDR V3.1 YSLF wind speeds from all CYGNSS satellites whose specular points are located near the storm of interest; lat–lon storm center estimates
Spatial range	Global (−180°:180° lon; ∓40° lat)	Moving grid; ±3.6° grid centered on storm center
Temporal range	Files output daily	Files output for individual storms, spanning the life cycle of the storm
Averaging coordinate system	Geographic coordinates	Storm-centric coordinates and polar coordinates
Latency	~6 days	Several months

Brought to you by UNIVERSITY OF MICHIGAN | Unauthenticated | Downloaded 03/06/23 02:27 PM UTC

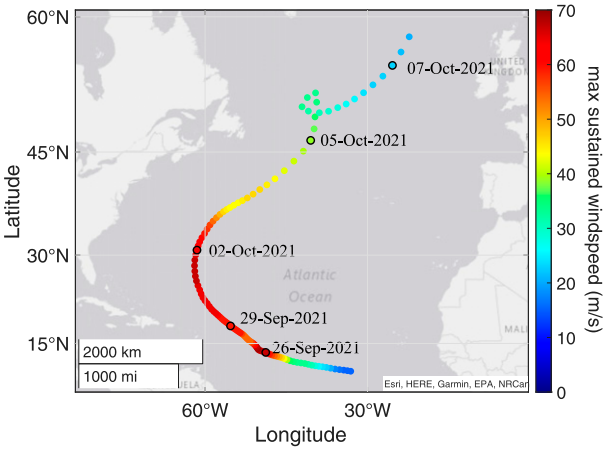


FIG. 10. TC best track and maximum sustained wind speed (V_{max}) of Hurricane Sam. Wind speed data are from the IBTrACS database (Knapp et al. 2010, 2018).

Next, the variation of the mean CYGNSS SP track wind speeds $\overline{\mu}_t$ is calculated to determine whether the spread of the 3+ CYGNSS SP tracks is typical. The expected standard deviation is computed from the relation

$$\sigma_{\text{Expected}} = 0.26\,x\,(\overline{u}_{\text{top2}} - 3.5), \tag{7}$$

where $\overline{u}_{\text{top2}}$ is the average of the two highest mean CYGNSS SP track wind speeds $\overline{\mu}_t$ after removal of outlier CYGNSS SP track(s). Equation (7) is derived from a best-fit line to data from the 2018 hurricane season, which is shown in Fig. 9. If the standard deviation of the mean CYGNSS SP track wind speeds is more than 3 m s^{-1} greater than the typical standard deviation estimated from Eq. (7), no wind speed is reported for the cell, that is,

$$\sigma_C^{-\text{Outliers}} > \sigma_{\text{Expected}} + 3 \text{ m s}^{-1}. \tag{8}$$

If the condition in Eq. (8) is not met, then the wind speed for the cell is reported as Eq. (3) but with outlier CYGNSS SP track(s) excluded.

Last, an inverse variance weighting scheme is used to average the samples remaining within a grid cell, consistent with the inverse variance weighting done on the standard L3 gridded wind speed products (Ruf 2018).

One additional difference between the L3 SCG products and the standard CYGNSS wind speed products is the data product latency. Because of the reliance on QC'd TC best-track information for the storm centric grid, the L3 SCG product latency is determined by the TC best-track data latency. This latency is typically on the order of several months after the conclusion of a TC season. As mentioned

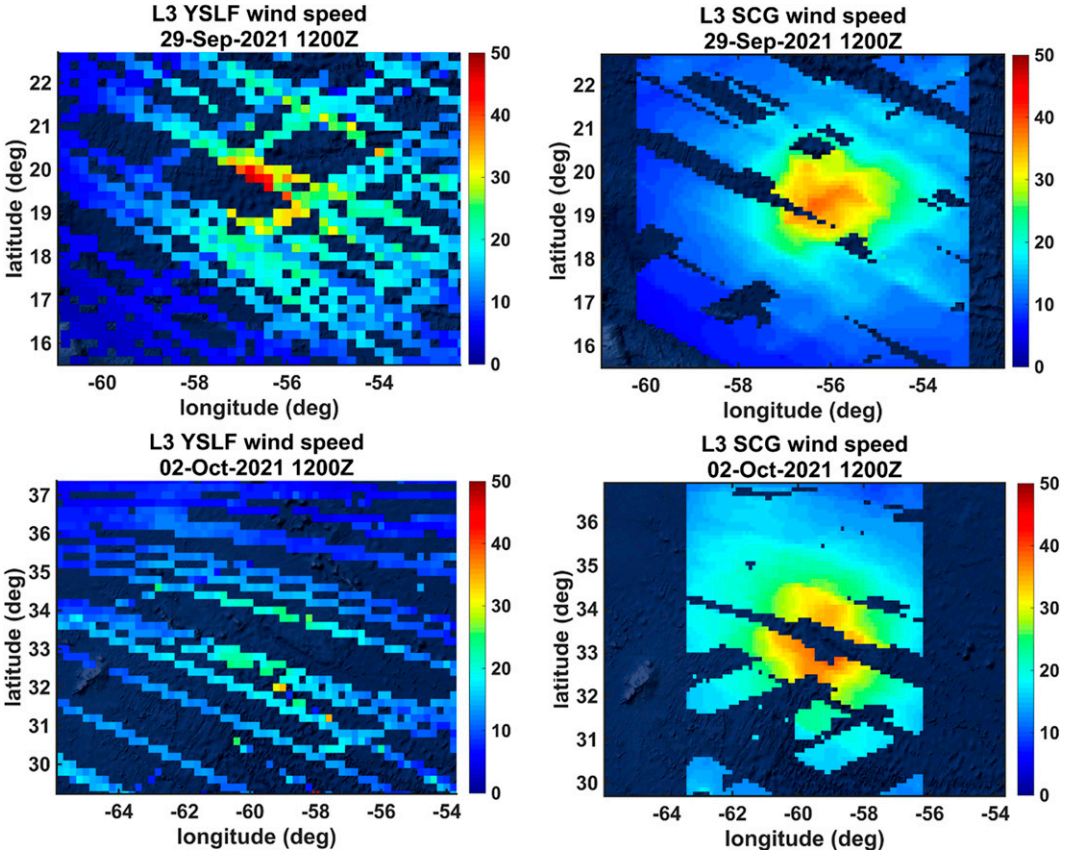


FIG. 11. (left) Examples of 12 h of CYGNSS L3 winds and (right) the L3 SCG wind fields covering the same time period for two Hurricane Sam wind fields.

Brought to you by UNIVERSITY OF MICHIGAN | Unauthenticated | Downloaded 03/06/23 02:27 PM UTC

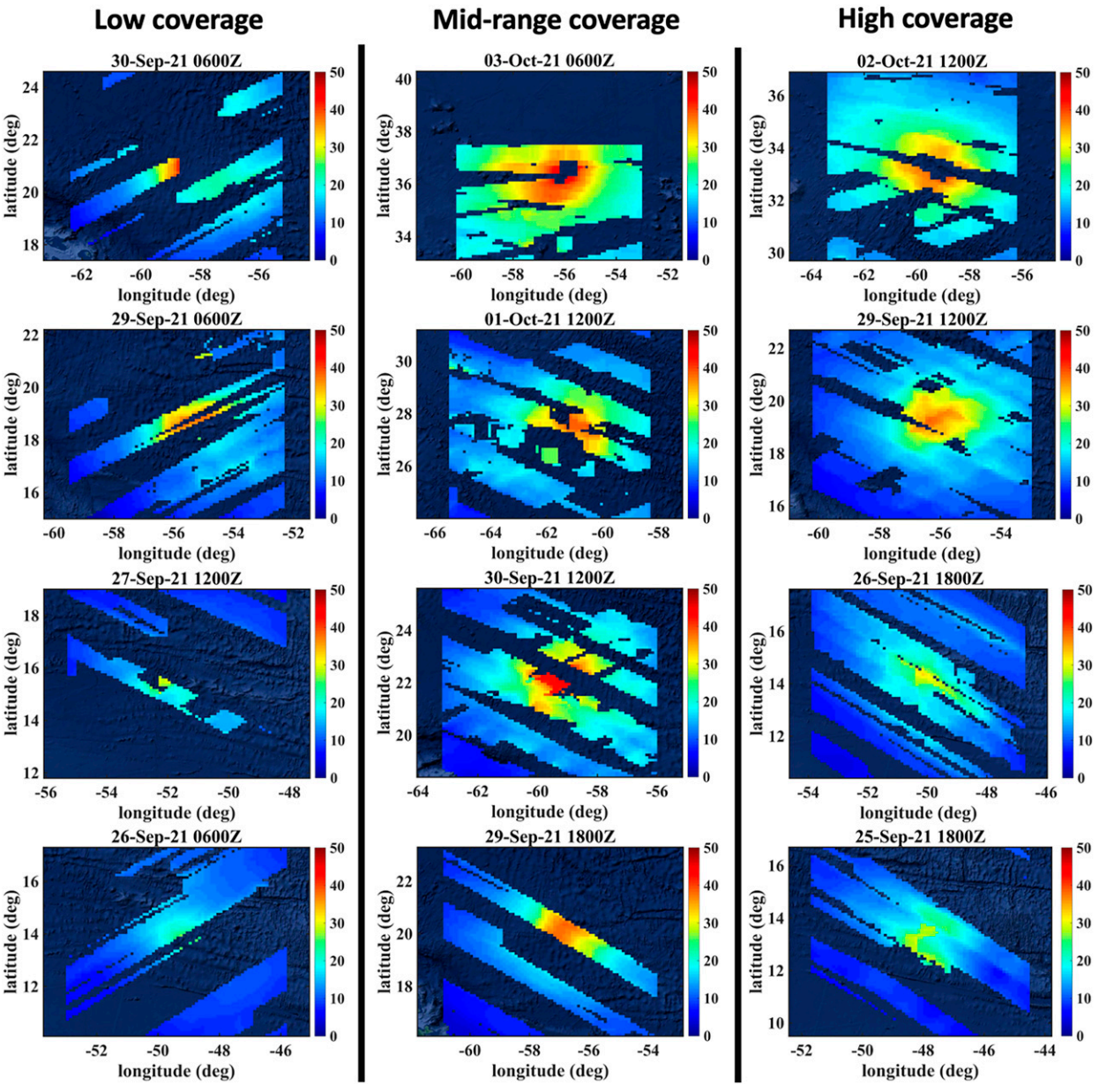


FIG. 12. Examples of L3 SCG surface wind fields (color shading; m s^{-1}) for Hurricane Sam, where there is (left) low, (center) midrange, and (right) high inner-core coverage.

above, L3 SCG files can also be generated using interim TC best-track data values for near-real-time applications, although these special data products are beyond the scope of this paper. A summary of the differences between the standard L3 wind speed product and the L3 SCG product is shown in Table 1.

3. Dataset examples

Examples of the L3 SCG wind products are demonstrated in this section for Hurricane Sam. This storm was chosen because it was an intense storm that had relatively good coverage by the CYGNSS constellation. Hurricane Sam was a category-4 storm that originated off the western coast of Africa in September 2021. Over a period of about 2 weeks, the storm underwent several cycles of intensification and weakening, reaching category-4 hurricane status first on 25 September, and again on 1 October. The storm subsequently weakened for good, dropping its hurricane status by 5 October and completely dissipating by 7 October. Because of its path, far from the U.S. eastern coast and at a safe distance from Bermuda (Fig. 10), the storm did not cause significant damage. Storms with trajectories far from land, like Sam's, are particularly difficult to collect data over since hurricane reconnaissance aircraft require a nearby

Brought to you by UNIVERSITY OF MICHIGAN | Unauthenticated | Downloaded 03/06/23 02:27 PM UTC

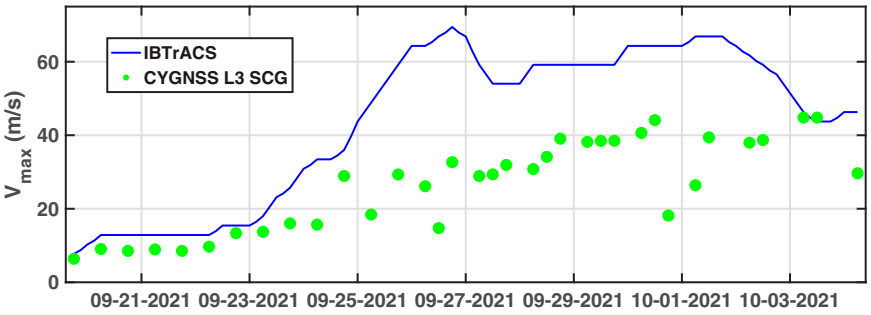


FIG. 13. Time series of the maximum Hurricane Sam wind speed reported in the IBTrACS database (blue line) and estimated by the CYGNSS L3 SCG wind fields (green dots).

airfield for missions. Figure 11 shows examples of ±6-hourly aggregated L3 YSLF winds for two time periods during Hurricane Sam's life cycle (left column) and the corresponding L3 SCG wind fields (right) that are the product of the L3 YSLF input winds with the QC and averaging applied in a storm-centric gridded coordinate system. Due to the motion of the storm, the aggregated L3 YSLF winds do not show a coherent wind field as expected, while the L3 SCG winds that have been averaged in a storm-centric gridded coordinate system reflect a more accurate structure of the storm wind field.

The L3 SCG wind fields shown in Fig. 11 contain good coverage of the storm's inner core (defined herein as the R34 radius); depending on the CYGNSS constellation's orbit during a storm's life cycle and the quality of the processed data, this coverage varies significantly. Figure 12 shows examples of wind fields over Sam's life cycle that contain low-, mid-, and high-inner-core coverage, defined as having ≤33%, 34%–66%, and ≥67% of the inner-core grid points containing values after the ±6 h aggregating and QC, shown in the left, center, and right columns, respectively. It can be seen that while some wind fields capture the overall structure of the inner core, other wind fields lack crucial data coverage either because of limited sampling or removal of these points during the QC process. Because of the unreliable coverage of the highest storm winds (in part because of the limited spatial resolution of the input L2 retrievals themselves) and the 12-h averaging of the wind speeds, the L3 SCG wind fields tend to underestimate the maximum wind speed whether the inner core is well sampled. This can be seen in Fig. 11 (top row), where the CYGNSS L3 YSLF wind product contains wind speeds between 40 and 50 m s^{-1}, while the corresponding L3 SCG wind field has a maximum wind speed around 38 m s^{-1}. Plotting the TC best-track-reported V_{max} alongside the maximum sustained wind speed in the L3 SCG wind fields for Hurricane Sam (Fig. 13) shows this discrepancy over the storm's life cycle, which is most notable when the storm's V_{max} is greater than 30–40 m s^{-1}. A fuller picture of the relationship between the CYGNSS L3 SCG wind fields and reported maximum sustained wind speed values is shown in Fig. 14. The scatterplot shows maximum wind speeds for all storm files over 2018–20 versus maximum sustained wind speeds reported by the NHC or JTWC (depending on the storm basin). The scatterplot is colored by log relative density so that overlying points are visually represented. Most points in the lower wind speed range (~8–17 m s^{-1}) have errors in the ±5 m s^{-1} range. As the observed maximum sustained wind speeds increase into the tropical storm/TC wind speed range, the errors develop a negative bias that range from an average of −10 to −60 m s^{-1} as the reported maximum sustained wind speeds increase from ~18 to 80 m s^{-1}. The algorithm likely is better able to match the lower maximum sustained wind speed measurements because there is less of a discrepancy between the TC and background winds during the initial growth phase when the wind field lacks organization, so the observed CYGNSS wind speeds are better able to represent the reported maximum sustained wind speeds regardless of the amount of spatial coverage of the TC wind field over a particular reporting interval.

While the L3 SCG data products are unreliable at capturing TC maximum sustained wind speeds in the core of fully

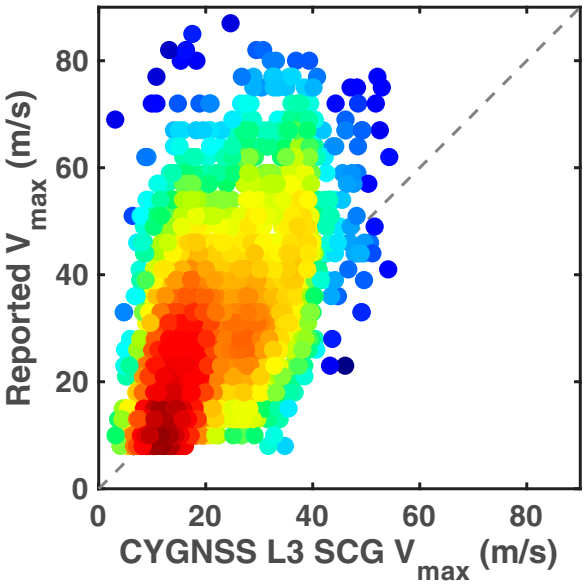


FIG. 14. Scatterplot of maximum wind speed observations in each CYGNSS L3 SCG wind field vs the reported maximum sustained wind speeds. Reported values are provided by the NHC or JTWC, depending on the basin. Plotted values are from the 2018–20 L3 SCG dataset.

Brought to you by UNIVERSITY OF MICHIGAN | Unauthenticated | Downloaded 03/06/23 02:27 PM UTC

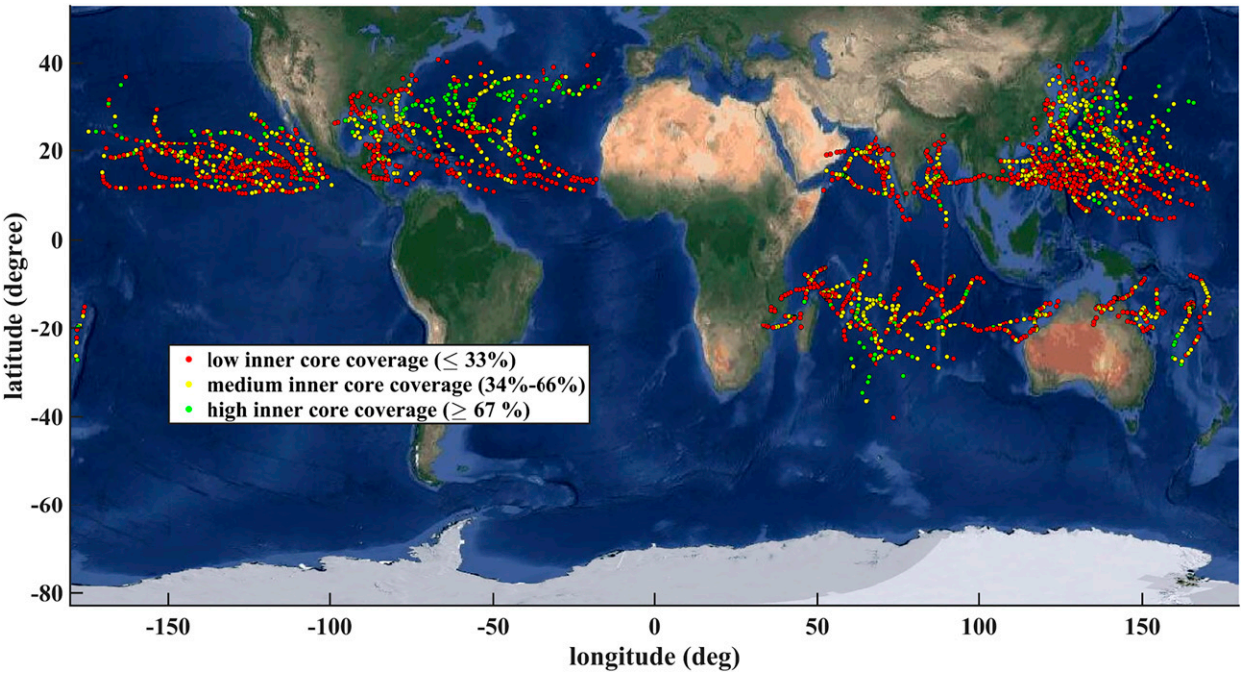


FIG. 15. Coverage of the L3 SCG database over 2018–20 storms. Each dot represents an L3 SCG wind field; the dots are colored by the percentage of the storm's inner core that is captured in the grid, where red, yellow, and green dots respectively represent ≤33%, 34%–66%, and ≥67% of the inner-core grid speeds containing an L3 SCG wind speed value.

developed storms, the ability of the L3 SCG data products to track lower intensity wind speeds in developing storms indicates the L3 SCG products could be useful for monitoring developing storms by running the algorithm with near-real-time TC track inputs in place of official TC track data. Additionally, the data product provides greater temporal coverage than comparable TC wind products (e.g., SMAP and AMSR). Figure 15 shows all available storms from 2018 to 2020, where each dot represents an L3 SCG wind field, color-coded by the inner-core coverage. While most of the wind fields fall into the "low" or "midrange" inner-core coverage categories, some degree of coverage is available at a 6-hourly interval for most storms, whereas existing TC wind products typically have complete lapses in data coverage on the order of days. The availability of sparse wind fields at a more frequent interval than existing TC wind products indicates the potential of using the L3 SCG wind products to provide general TC wind speed data informing background/initial wind fields (e.g., assimilation for TC reanalysis/hindcasts), where the lack of accurate V_{max} data may not hinder the overall simulation.

4. Summary and conclusions

A new gridded CYGNSS wind speed product has been developed for representing tropical cyclone surface wind speeds. The L3 SCG product increases the spatial coverage of CYGNSS gridded wind speeds over the standard L3 gridded wind speed products by aggregating the CYGNSS L2 YSLF wind speeds over a ±6-h window, on a standardized, moving grid that collocates measurements taking the storm's forward motion into account. This approach allows for a more complete representation of the storm winds at a given time, as compared with the standard L2 and L3 wind speed products. Caveats to this product are that the longer averaging window will not capture rapid intensification or decay events, and the algorithm's reliance on TC best-track geolocation data makes it unsuitable for forecasts as its latency is on the order of months. Additionally, while a more complete storm is represented in the L3 SCG files, the sporadic nature of the CYGNSS measurements combined with the 12-h averaging window and QC leads to the L3 SCG product typically underestimating the maximum wind speeds in a TC. One possibility for mitigating these shortcomings for future GNSS-R based TC products would be to have a greater number of satellites in orbit to increase spatial coverage and reduce the required averaging window. Despite these caveats, the L3 SCG wind speed products have greater temporal availability than existing TC wind products and may be beneficial for applications where frequent measurements of background TC wind fields are needed. Additionally, the L3 SCG product shows promise for tracking storm behavior during initial development from a tropical disturbance to a tropical storm and could shed light on these processes. Future iterations of the L3 SCG dataset will include expanding the TC storm centered grid beyond ±3.6° to capture more TC features, as well as implementing a near-real-time data product that uses inputs from interim TC center location data sources.

Acknowledgments. This research was supported in part by National Aeronautics and Space Administration (NASA)

Brought to you by UNIVERSITY OF MICHIGAN | Unauthenticated | Downloaded 03/06/23 02:27 PM UTC

Science Mission Directorate contracts NNL13AQ00C and 80LARC21DA003 with the University of Michigan.

Data availability statement. All CYGNSS data created or used during this study are openly available from the NASA Physical Oceanography Distributed Active Archive Center (https://podaac-tools.jpl.nasa.gov/drive/files/allData/cygnss).

REFERENCES

Al-Khaldi, M. M., J. T. Johnson, Y. Kang, S. J. Katzberg, A. Bringer, E. Kubatko, and D. Wood, 2020: Track-based cyclone maximum wind retrievals using the Cyclone Global Navigation Satellite System (CYGNSS) mission full DDMs. *IEEE J. Sel. Top. Appl. Earth Obs. Remote Sens.*, **13**, 21–29, https://doi.org/10.1109/JSTARS.2019.2946970.

Cui, Z., Z. Pu, V. Tallapragada, R. Atlas, and C. S. Ruf, 2019: A preliminary impact study of CYGNSS ocean surface wind speeds on numerical simulations of hurricanes. *Geophys. Res. Lett.*, **46**, 2984–2992, https://doi.org/10.1029/2019GL082236.

Knapp, K. R., M. C. Kruk, D. H. Levinson, H. J. Diamond, and C. J. Neumann, 2010: The International Best Track Archive for Climate Stewardship (IBTrACS): Unifying tropical cyclone best track data. *Bull. Amer. Meteor. Soc.*, **91**, 363–376, https://doi.org/10.1175/2009BAMS2755.1.

——, H. J. Diamond, J. P. Kossin, M. C. Kruk, and C. J. Schreck, 2018: International Best Track Archive for Climate Stewardship (IBTrACS) project, version 4. NOAA National Centers for Environmental Information, accessed 26 June 2020, https://doi.org/10.25921/82ty-9e16.

Landsea, C. W., and J. L. Franklin, 2013: Atlantic hurricane database uncertainty and presentation of a new database format. *Mon. Wea. Rev.*, **141**, 3576–3592, https://doi.org/10.1175/MWR-D-12-00254.1.

Li, X., J. R. Mecikalski, and T. J. Lang, 2020: A study on assimilation of CYGNSS wind speed data for tropical convection during 2018 January MJO. *Remote Sens.*, **12**, 1243, https://doi.org/10.3390/rs12081243.

Mueller, M. J., B. Annane, S. M. Leidner, and L. Cucurull, 2021: Impact of CYGNSS-derived winds on tropical cyclone forecasts in a global and regional model. *Mon. Wea. Rev.*, **149**, 3433–3447, https://doi.org/10.1175/MWR-D-21-0094.1.

Pascual, D., M. P. Clarizia, and C. S. Ruf, 2021: Improved CYGNSS wind speed retrieval using significant wave height correction. *Remote Sens.*, **13**, 4313, https://doi.org/10.3390/rs13214313.

Ruf, C. S., 2018: Cyclone Global Navigation Satellite System (CYGNSS): Algorithm theoretical basis document level 3 gridded wind speed. University of Michigan (UM) Doc. 148-0319, 10 pp., https://cygnss.engin.umich.edu/wp-content/uploads/sites/534/2021/07/148-0319-ATBD-L3-Gridded-Wind-Speed_Rev1_Aug2018_release.pdf.

——, and R. Balasubramaniam, 2019: Development of the CYGNSS geophysical model function for wind speed. *IEEE J. Sel. Top. Appl. Earth Obs. Remote Sens.*, **12**, 66–77, https://doi.org/10.1109/JSTARS.2018.2833075.

——, C. Chew, T. Lang, M. G. Morris, K. Nave, A. Ridley, and R. Balasubramaniam, 2018: A new paradigm in Earth environmental monitoring with the CYGNSS small satellite constellation. *Sci. Rep.*, **8**, 8782, https://doi.org/10.1038/s41598-018-27127-4.

——, S. Asharaf, R. Balasubramaniam, S. Gleason, T. Lang, D. McKague, D. Twigg, and D. Waliser, 2019: In-orbit performance of the constellation of CYGNSS hurricane satellites. *Bull. Amer. Meteor. Soc.*, **100**, 2009–2023, https://doi.org/10.1175/BAMS-D-18-0337.1.

Brought to you by UNIVERSITY OF MICHIGAN | Unauthenticated | Downloaded 03/06/23 02:27 PM UTC